Time-Domain Synthesis of Broad-Band Absorptive Coatings for Two-Dimensional Conducting Targets

MARK A. STRICKEL, MEMBER, IEEE, AND ALLEN TAFLOVE, FELLOW, IEEE

Abstract—**A new time-domain synthesis approach is introduced for broad-band absorptive coatings suitable for radar cross section (RCS) management. The new algorithm involves a finite-difference time-domain (FD-TD) forward-scattering represention of Maxwell's curl equations in a numerical feedback loop with the Levenberg–Marquardt (L-M) nonlinear optimization routine. L-M is used to adjust many geometric and constitutive parameters that characterize a target, while FD-TD is used to obtain the broad-band bistatic RCS response for each target adjustment. A recursive improvement process is established to minimize the broad-band RCS response over a selected range of bistatic angles using the available engineering degrees of freedom. The solution is valid over the potentially broad bandwidth (frequency decade or more) of the illuminating pulse used in the FD-TD computational model. Examples of this method are provided in the area of RCS management for canonical two-dimensional conducting targets.**

I. INTRODUCTION

SYNTHESIS PROBLEMS are of fundamental importance in electrical engineering. In electromagnetics, essentially all the existing synthesis approaches utilize frequency-domain forward data, i.e., sinusoidal steady-state values for radiated or scattered fields, reflection coefficients, etc. Synthesis over a broad frequency band, therefore, requires calculations spread over the desired band and over the range of the engineering degrees of freedom in the design. In the area of radar cross section (RCS) management, this synthesis approach has driven research in reducing computer resource burdens involved in executing frequency-domain forward-scattering codes.

This paper introduces a new time-domain synthesis approach for broad-band absorptive coatings suitable for RCS management. The new algorithm involves a finite-difference time-domain (FD-TD) forward-scattering representation of Maxwell's curl equations [1] in a numerical feedback loop with the Levenberg–Marquardt (L-M) nonlinear optimization routine [2]. L-M is used to adjust many geometric and constitutive parameters that characterize a target, while FD-TD is used to obtain the broad-band bistatic RCS response for each target adjustment. A recursive improvement process is established to minimize the broad-band RCS response over a selected range of bistatic angles using the available engineering degrees of freedom. The solution is valid over the potentially broad bandwidth (frequency decade or more) of the illuminating pulse used in the FD-TD computational model.

Because the FD-TD forward element is a direct solution of Maxwell's curl equations, it models in a straightforward manner a wide variety of electromagnetic wave scattering and interaction phenomena. The accuracy of FD-TD modeling is equivalent to that of the widely used, frequency-domain method of moments (MM), with essentially equivalent results of the two methods for arbitrary conducting and penetrable targets (the latter having media properties as complex as diagonalizable tensors) [1], [3], [4]. However, the explicit nature of the FD-TD algorithm leads to computer storage and running time burdens that are dimensionally low compared to those of MM for targets that are either electrically large or have a complex, inhomogeneous material composition. The accuracy and efficiency of FD-TD, combined with its time-domain formulation which allows direct modeling of broad-band phenomena, makes FD-TD the algorithm of choice for the forward-scattering element of the new time-domain synthesis approach.

The L-M algorithm [2], selected for use in the feedback path, is also considered to be robust and one of the best optimization methods for nonlinear least-squares problems. A good example of the utility of L-M optimization as opposed to possible alternatives such as the quasi-Newton method and the conjugate gradient method is given in [5], which reports the synthesis of near-field patterns using linear arrays of point dipoles. It is shown in [5] that L-M is the most effective synthesis algorithm in this application.

This paper describes the new FD-TD/L-M synthesis method, and provides examples of its application to synthesize absorptive coatings for broad-band RCS management of canonical two-dimensional (2-D) conducting targets. The new method is used to synthesize both isotropic and anisotropic coatings for three target shapes: 1) the infinite, flat metal plate illuminated at normal incidence; 2) the infinite right-angle metal wedge; and 3) the infinitely long circle-capped (rounded) metal strip of finite thickness. In each example, the synthesized absorptive coating is assumed to be nondispersive. However, it appears possible to incorporate canonical dispersions into the FD-TD element. This will be a subject of later work.

Manuscript received March 2, 1989; revised June 21, 1989. This work was supported in part by National Science Foundation Grant ASC-8811273 and by the Office of Naval Research under Contract N00014-88-K-0475.

M. A. Strickel is with Geldermann, Inc., 440 South LaSalle, Chicago, IL 60605.

A. Taflove is with the Electrical Engineering and Computer Engineering Department, McCormick School of Engineering, Northwestern University, Evanston, IL 60208-3118.

IEEE Log Number 9035920.

II. FD-TD/L-M Algorithm

In this section, we discuss the application of the FD-TD/L-M algorithm to the synthesis of broad-band absorptive coatings for RCS management. For simplicity, we shall consider a target of fixed shape and size, although the synthesis algorithm is so general that optimization of target geometrical features can be incorporated in a straightforward manner.

We first observe that the properties of a target's coating can be described by a set of key parameters. These parameters might include the number of layers in the coating, the thickness of each layer, the components of the constitutive tensors of each layer (electrical permittivity and conductivity, as well as magnetic permeability and loss), and finally the variation of the previous properties with position along the target surface. It is clear that the number N of key parameters can be large: effectively, there are N degrees of freedom. For purposes of this synthesis approach, it is very useful to consider the state of the overall coating as a single point in an N-dimensional space defined by a coordinate value for each degree of freedom. The optimum coating can be synthesized by efficiently searching N-space for the set of points (hopefully not the empty set) that satisfies the engineering criteria.

The FD-TD/L-M synthesis algorithm begins with an initial guess for the target coating properties, i.e., a starting point in the N-space discussed above. The FD-TD element computes scattered field-versus-time waveforms at the desired set of physical locations in the near or far field. (The latter are calculated using a time-domain analog of the near-to-far-field transformation discussed in [6].) FD-TD computations of the scattered transient responses at the locations of interest are compared to the desired field waveforms at these points. For comparison points in the backscatter direction, RCS management goals may dictate that the desired scattered field waveform is simply zero, and the mere presence of a calculated transient scattered response at these points comprises an error signal. More generally, the FD-TD calculated scattered pulse responses at all observation points of interest are compared to the desired time profiles, and a weighted, composite error signal is generated, which is sent to the L-M nonlinear optimization feedback element, as shown in Fig. 1(a). The L-M routine adjusts the position of the operating point in the coating N-space in a direction to reduce the error signal in the least-squares sense. With the calculation process in the time domain, causality can be exploited in the optimization process to modify only the coating properties causally connected to the physical observation points, thereby windowing desired target features.

With the version of the L-M algorithm used here, the N-space search per iteration through the FD-TD/feedback loop is conducted in two phases. In Phase 1, the search direction is established by calculating partial derivatives of the error signal with respect to each of the N dimensions (degrees of freedom). If central differences are used, two forward FD-TD runs are required per degree of freedom for this purpose, so that this phase entails $2N$ FD-TD runs. In Phase 2, a line search is conducted along the calculated search direction to determine the distance that the operating point moves in the

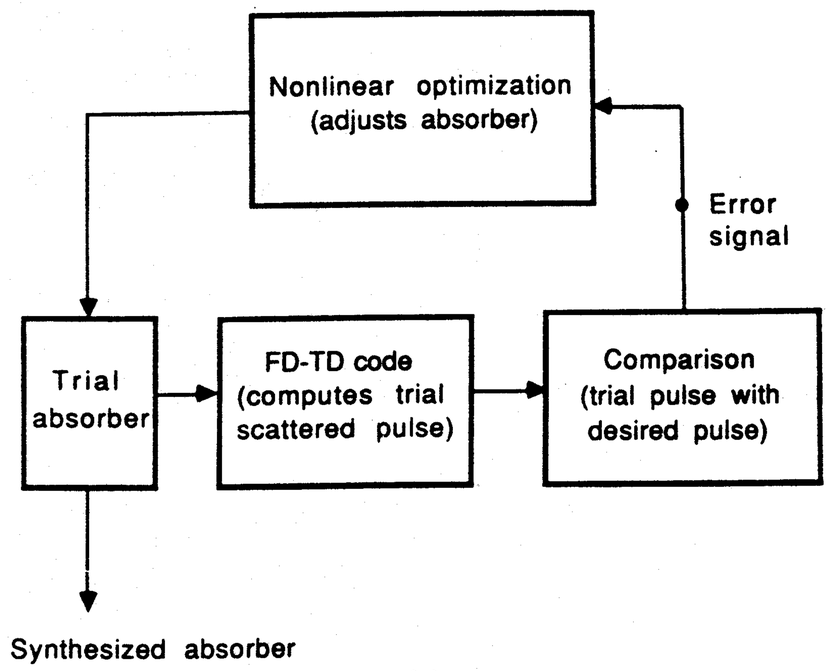

Fig. 1. FD-TD/feedback method for electromagnetic absorber synthesis. (a) Block diagram. (b) Energy spectral density of the one-half cycle, 3-GHz sinusoidal pulse used as the illuminating waveform.

N-space. Numerical experiments indicate that approximately ten additional forward FD-TD runs are needed for this phase. At this juncture in the algorithm, the new operating point in the coating N-space has been established.

This process is repeated until the error signal drops to some minimum value which shows no further reduction upon additional iterations. Effectively, the procedure traces out a path in the coating N-space from the initial guess or starting point to the final coating state. The recursive improvement process established for the coating in this manner leads at worst to a local minimization of the error, that is, local in the sense of the coating N-space. Without much doubt, there may exist a number of such local minima, and possibly even a global error minimum for the entirety of the N-space. A challenging aspect of the nonlinear optimization process is to develop efficient means to perform a global search of the coating N-space. One possible approach is the use of advanced multiprocessing computers such as the Connection Machine to implement concurrently a large number of search trajectories in the coating N-space, seeded by a like number of starting points. Research in this area is commencing.

With the L-M optimization algorithm providing an efficient means of searching through the coating N-space, it becomes possible to either: 1) add additional degrees of freedom, i.e., dimensions to the N-space, to permit the target shape to be optimized as well; or 2) to define forbidden zones in the N-space through which search trajectories cannot pass due to

constraints imposed by manufacturing costs, material availability, or any other factors. Thus, the optimization for electromagnetic properties can be treated as a subset of a more general optimization wherein systems-type considerations can be imposed.

III. Synthesis Example in One Dimension

This section provides a simple example of the use of the FD-TD/L-M method: synthesis of a broad-band, two-layer absorbing coating to mitigate reflection of a normally incident plane wave by an infinite, planar, perfectly conducting sheet. For this (and subsequent) examples, it is desired merely to indicate the potential of this approach without actually completing an engineering design for scattering mitigation, so the number of design degrees of freedom is kept small. Further, artificial constraints are imposed upon the constitutive parameters of the absorber to avoid undue realism. For this example, the following constraints are imposed:

1) Overall absorber thickness—10 mm
2) Number of absorber layers—two
3) Properties of inner layer (next to conducting sheet)
   thickness—7.5 mm
   free-space permittivity
   finite electric and magnetic conductivities, σ_e and σ_m
   electrical conductivity equal to that of the outer layer
4) Properties of outer layer
   thickness—2.5 mm
   free-space permittivity and permeability
   only electric loss is present, and this is equal to that of the inner layer.

Thus, it is seen that the coating N-space has a dimensionality of only three, with the inner/outer layer electric loss, inner-layer magnetic permeability, and inner-layer magnetic loss the only design degrees of freedom available.

The absorber-coated conducting sheet is synthesized using a 50-cell, one-dimensional FD-TD grid having a uniform cell size of 0.5 mm. The broad-band excitation is a one-half cycle 3-GHz sinusoidal pulse having the energy spectral density shown in Fig. 1(b). Note that the exciting pulse has substantial energy content from dc to over 5 GHz, and that minimization of the reflected time-domain waveform in the least-squares sense amounts to a very broad-band mitigation of scattering.

To begin the synthesis process, the point ($\sigma_e = 0.5$ S/m, $\mu_r = 2.0$, $\sigma_m = 0.5\eta_0^2$ Ω/m) in the coating three-space is selected arbitrarily as an initial guess, where η_0 is the characteristic impedance of free space. While tracing out a trajectory in the coating three-space from this starting point, the FD-TD/feedback algorithm is constrained to keep the electric and magnetic conductivity values nonnegative and the permeability greater than or equal to one. For this example, causality is not exploited in the optimization and the entirety of the reflected pulse is considered as the error signal to be minimized in the least-squares sense. It is found that six-passes through the FD-TD/feedback system are needed for convergence, with each pass requiring 16 FD-TD runs (each 350 time steps). At the conclusion of this process, which involves a total CPU time of 2 min on the VAX 11/780, the operating point in the coating three-space has shifted to (0.4632, 4.497, $1.336\eta_0^2$), and the error signal (energy in the reflected time-domain waveform) has been reduced by a factor of 134:1 from that of the initial guess for the coating.

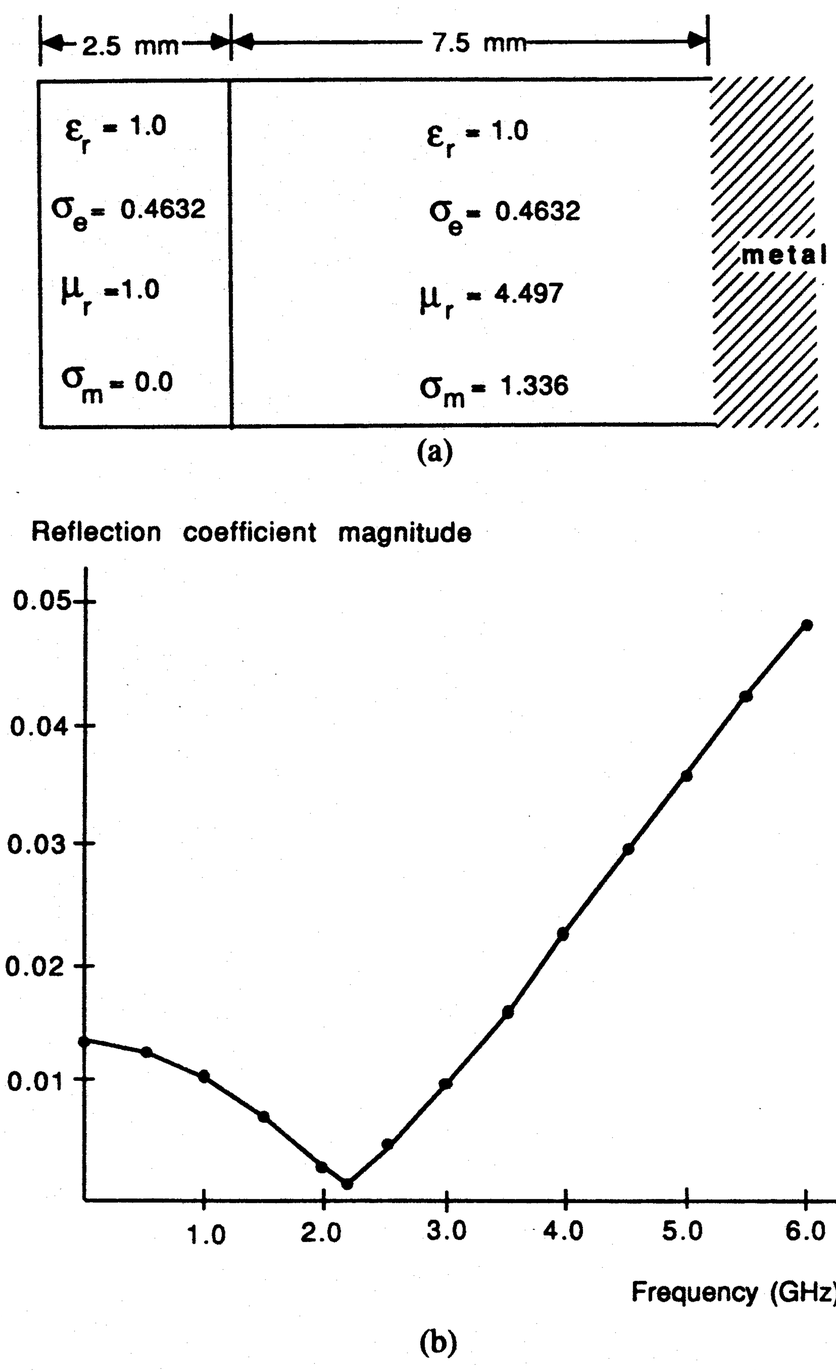

Fig. 2. Synthesis example in one dimension. (a) Final coating state after convergence of the synthesis algorithm. (b) Reflection coefficient magnitude versus frequency for the synthesized coating over metal.

Fig. 2(a) shows the final coating state after convergence of the synthesis algorithm. (For notational simplicity in this and later examples, the listed value of magnetic conductivity is the actual value divided by η_0^2.) Validation of the effectiveness of this procedure is provided in Fig. 2(b), which plots as a function of frequency the usual sinusoidal-wave reflection coefficient for the coated conducting sheet, calculated using standard impedance-transformation formulae applied to the synthesized coating. Over the frequency range 0–6 GHz, this reflection coefficient is less than 0.05 (−26 dB), achieving a minimum value of 0.0014 (−57 dB) at 2.2 GHz.

IV. Synthesis of Absorptive Coatings for the Infinite Metal Wedge

In this section, the FD-TD/feedback method is used to synthesize absorbing coatings for an important canonical two-dimensional structure, the infinite, perfectly conducting, right-angle wedge subject to transverse magnetic (TM) plane-wave illumination. As in the previous example, constraints are placed upon the synthesis to indicate the potential of the approach without completing an actual engineering design.

Fig. 3 shows the constraints imposed upon the problem to meet the above goals. The wedge, shown as the shaded region

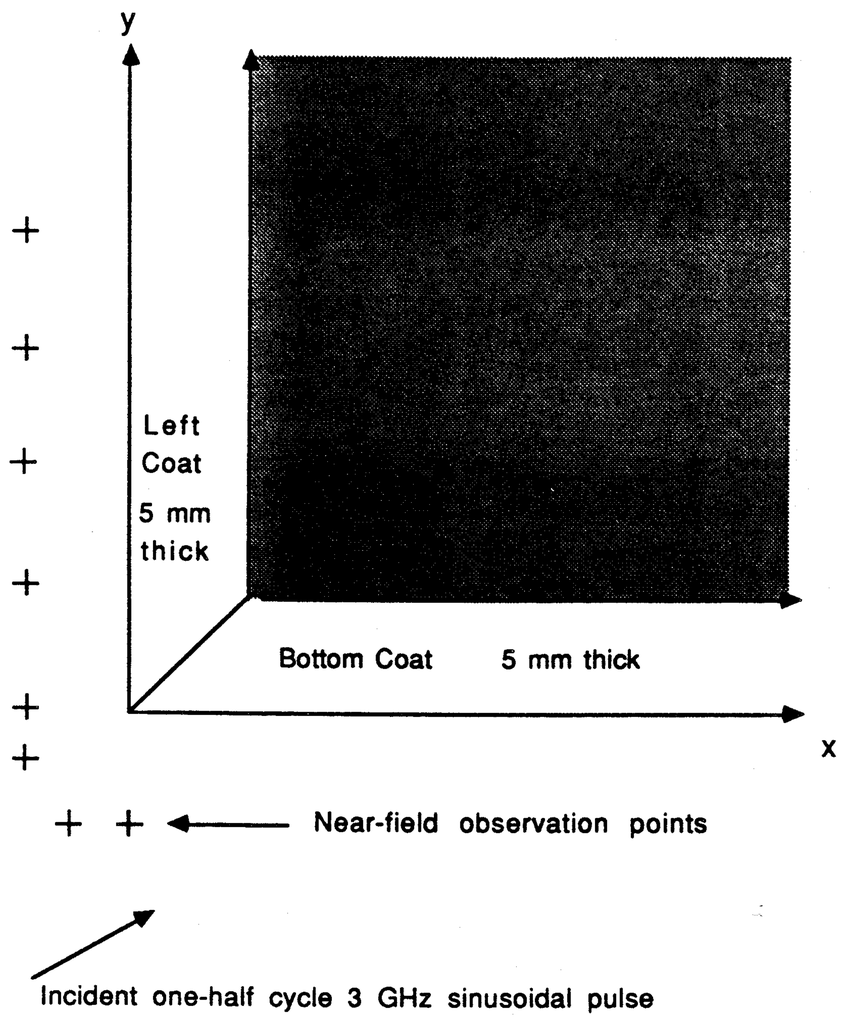

Fig. 3. Assumed geometry for the synthesis of absorbing coatings on an infinite, perfectly conducting, right-angle wedge.

extending an infinite distance along the $+x$ and $+y$ axes, is assumed coated with two distinct, homogeneous absorbers: a 5-mm thick "left" coat along the $+y$-axis; and a 5-mm thick "bottom" coat along the $+x$-axis. The two coats are in contact at the wedge vertex and form a miter joint. Two different coating pairs are synthesized. In Case 1, the left and bottom coats are isotropic; while in Case 2, the left and bottom coats have diagonal tensor anisotropy for the magnetic loss. For both cases, the relative permittivity and permeability of the coats is assumed fixed at 1.0 (a scalar value); the left-coat electrical conductivity is fixed at 1.25 S/m (scalar); and the bottom-coat electrical conductivity is fixed at 0.5 S/m (scalar). Thus, for Case 1, the coating N-space has a dimensionality of only two (the left- and bottom-coat scalar magnetic losses being the only degrees of freedom); while for Case 2, the coating N-space has four dimensions (the two diagonal tensor components of magnetic loss for each of the two coats).

The coated wedge is synthesized using a 200×300 cell two-dimensional FD-TD grid having a uniform cell size of 0.5 mm. The broad-band excitation is again a one-half cycle, 3-GHz sinusoidal pulse, TM polarized, and having an incident wavevector oriented at 30° with respect to the $+x$-axis. Time waveforms of the scattered electric near field are observed at eight points located 5 mm from the coated wedge, denoted by "+" signs in Fig. 3. By properly selecting the FD-TD grid and wedge size, as well as the number of time steps, the observation points are causally isolated from diffraction effects at the rear of the wedge for a length of time sufficient to permit the observed fields to decay as they would for an infinite wedge. (In effect, the time-domain formulation of the forward-scattering element is exploited to permit effective simulation of an infinite wedge by time-gating spurious diffraction effects due to finite actual wedge size [7].) The error signal input to the optimizer consists of the square of the sum of the absolute values of the FD-TD computed time samples at the eight observation points, accumulated time-step by time-step until the essential decay of the computed fields at the observation points.

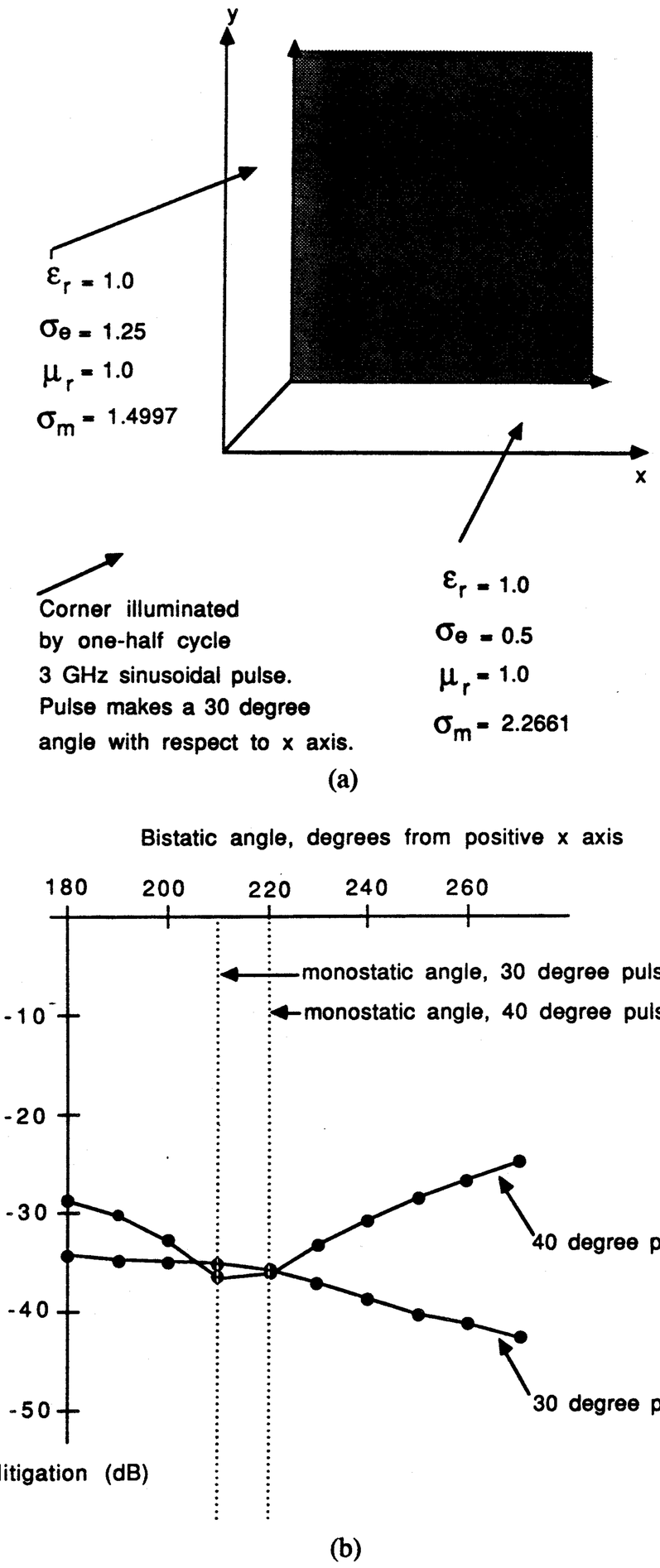

Fig. 4. Synthesis results for the conducting right-angle wedge, isotropic coating case. (a) Final coating state after convergence of the synthesis algorithm. (b) Mitigation of the broad-band scattered pulse in the far field versus bistatic angle.

To begin the synthesis process for the isotropic coatings of Case 1, the point ($\sigma_{m_{\text{left}}} = 1.25$, $\sigma_{m_{\text{bot}}} = 5.0$) in the coating two-space is selected arbitrarily as the initial guess. It is found that six passes through the FD-TD/feedback system are needed for convergence, with each pass requiring 14 FD-TD runs (each 350 time steps). At the conclusion of this process, which involves a total CPU time of 2 min on a single processor of the Cray X-MP, the operating point in the coating two-space has shifted to (1.50, 2.266), and the error signal has been reduced by a factor of 2.9 : 1 from that of the initial guess for the coating.

Fig. 4(a) shows the final coating state for Case 1 after convergence of the synthesis algorithm, and Fig. 4(b) shows the corresponding mitigation of the broad-band scattered pulse in

the far field. The mitigation, shown over the bistatic angular range 180°–270°, is a broad-band figure of merit defined here as the ratio of the peak amplitudes of the computed scattered pulses for the absorber-coated and uncoated wedge. From Fig. 4(b), we see that the calculated bistatic mitigation for the 30° incident pulse used in the synthesis is fairly flat (ranging from −35 to −42 dB), with a mitigation of −37 dB for the broad-band monostatic return at 210°. To illustrate the sensitivity of the mitigation to the illumination angle, Fig. 4(b) also shows results for the same coating state but with the incident pulse rotated by 10° in azimuth (propagating at 40° with respect to the $+x$-axis). The new monostatic return at 220° shows little change from the previous value. However, there appears to be somewhat degraded bistatic mitigation at angles to either side of 220°.

To begin the synthesis process for the anisotropic coatings of Case 2, the point ($\sigma_{m_x,\text{left}} = 0.1$, $\sigma_{m_y,\text{left}} = 1.34$, $\sigma_{m_x,\text{bot}} = 6.92$, $\sigma_{m_y,\text{bot}} = 0.5$) in the coating four-space is selected arbitrarily as the initial guess. It is found that 15 passes through the FD-TD/feedback system are needed for convergence, with each pass requiring 18 FD-TD runs (each 350 time steps). At the conclusion of this process, which involves a total CPU time of 6.4 min on a single processor of the Cray X-MP, the operating point in the coating four-space has shifted to (0.01, 1.604, 2.24, 0.0174), and the error signal has been reduced by a factor of 205:1 from that of the initial guess for the coating.

Fig. 5(a) shows the final coating state for Case 2 after convergence of the synthesis algorithm, and Fig. 5(b) shows the corresponding mitigation of the broad-band scattered pulse in the far field. From Fig. 5(b), we see that the calculated bistatic mitigation for the 30° incident pulse used in the synthesis varies in the range −44 dB to −60 dB, with a mitigation of −53 dB for the broadband monostatic return at 210°. This is an improvement of 16 dB relative to the isotropic coatings of Case 1. However, the sensitivity of the mitigation to illumination angle appears increased for Case 2 relative to Case 1. This is indicated by the results shown in Fig. 5(b) for the same anisotropic coating state but with the incident pulse rotated by 10° in azimuth to propagate at 40° with respect to the $+x$-axis. The new monostatic return at 220° is degraded to a −43 dB mitigation, and the remainder of the bistatic mitigation pattern generally is degraded even more.

In viewing the results for Case 2, one might conclude that anisotropic coatings present some difficulties with respect to scattering mitigation over a useful range of illumination angles. However, this conclusion is not warranted. Case 2 shown here was purposefully selected to represent a coating space of low dimensionality (no layering, no variation of permittivity or permeability, etc.). Our preliminary work has shown that synthesis of scattering mitigation over a specified range of illumination angles is possible for Case 2 simply by permitting more degrees of freedom.

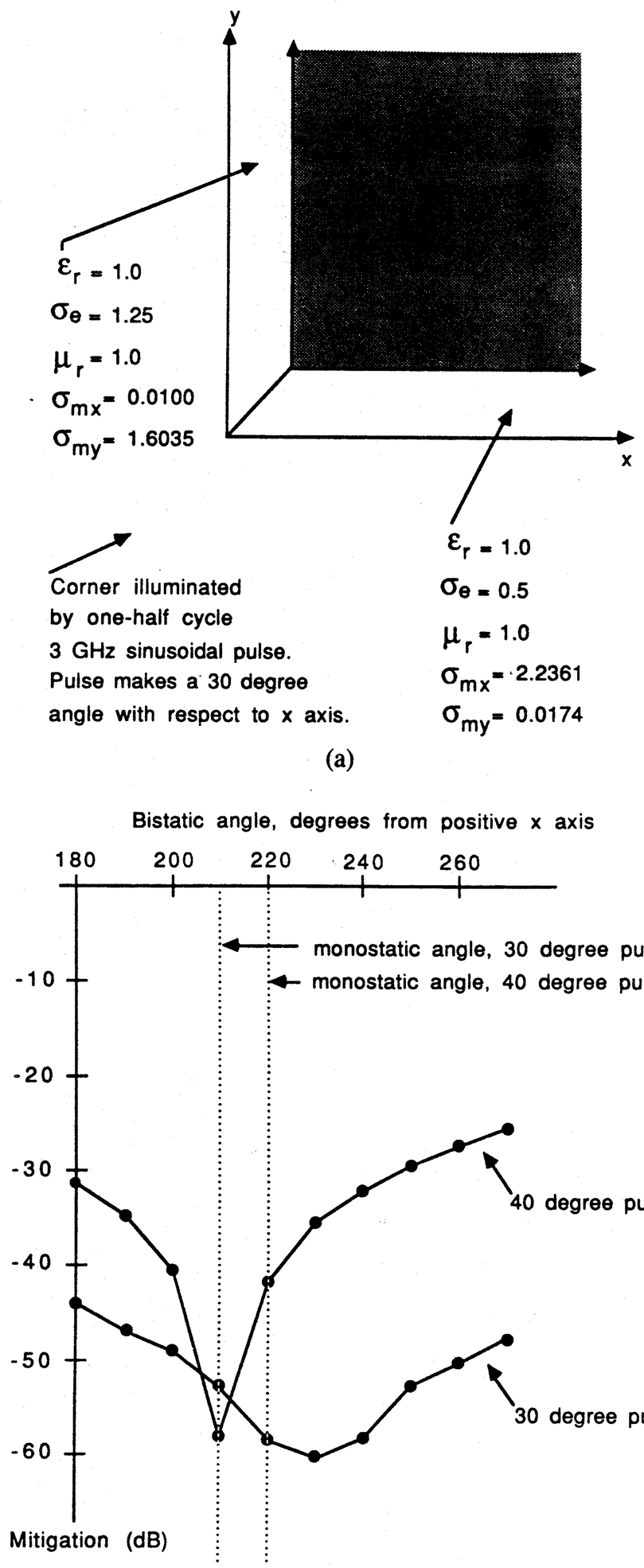

Fig. 5. Synthesis results for the conducting right-angle wedge, anisotropic coating case. (a) Final coating state after convergence of the synthesis algorithm. (b) Mitigation of the broad-band scattered pulse in the far field versus bistatic angle.

V. Synthesis of Absorptive Coatings for the Rounded Metal Strip

In this section, the FD-TD/feedback method is used to synthesize absorbing coatings for a second canonical two-dimensional structure, the infinitely long, perfectly conducting strip of finite thickness having a semicircular rounded edge. (This is the two-dimensional analog of the infinitely-long, sphere-capped cylinder.) As in the previous examples, the dimensionality of the coating space is deliberately kept low.

Fig. 6 shows the constraints imposed upon the problem to meet the above goal. The rounded strip, shown as the shaded region extending an infinite distance and centered along the $+x$-axis, is assumed to be 10 mm thick and coated with a 5-mm thick absorber. The absorber is assumed to be comprised of distinct 0.5-mm thick layers, with each layer parallel to the x-axis and having homogeneous material properties. Even symmetry of the absorber properties is assumed about the x-

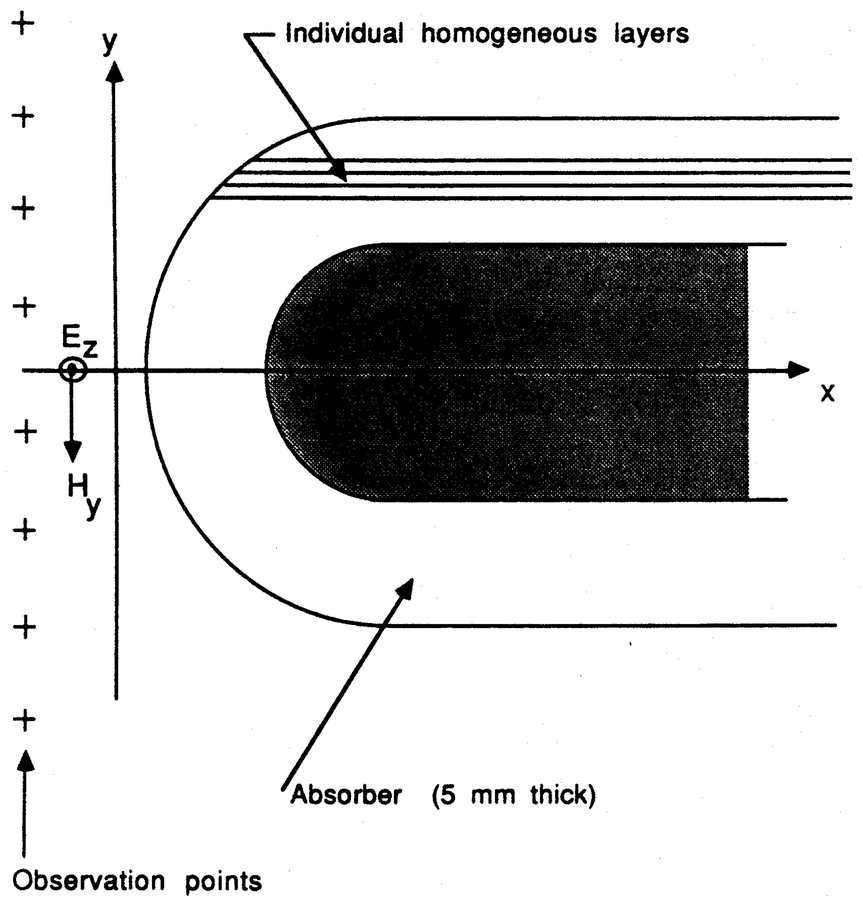

Fig. 6. Assumed geometry for the synthesis of absorbing coatings on an infinite, perfectly conducting strip of finite thickness with rounded edge.

axis. For notational simplicity, the coating layers to either side of the x-axis are assigned the indices $j = 0.1, 0.2, \cdots, 2.0$, where the $j = 2.0$ layer is farthest from the x-axis. Given this arrangement, two different coatings are synthesized.

Case 1: Each coating layer is assumed to be isotropic, and the electric and magnetic conductivities are assumed to be separate, nonnegative, quadratic functions of the "j" index of the layer, defined by

$$\sigma_e(j) = |a_0 + a_1 j + a_2 j^2|;$$

$$\sigma_{m_x}(j) = \sigma_{m_y}(j) = |b_0 + b_1 j + b_2 j^2|.$$

Case 2: Each coating layer is assumed to be anisotropic, with the electric and magnetic conductivities defined as a function of the layer "j" index by the nonnegative quadratic functions

$$\sigma_e(j) = \sigma_{m_y}(j) = |c_0 + c_1 j + c_2 j^2|;$$

$$\sigma_{m_x}(j) = |d_0 + d_1 j + d_2 j^2|.$$

For both cases, the relative permittivity and permeability for each coating layer is assumed to be one. Thus, despite the large number of layers in the absorber for each case, the coating N-space has a dimensionality of only six because there are only six degrees of freedom implied by the three coefficients for each of two quadratic functions used to describe the overall absorber electrical characteristics.

The coated, rounded strip is synthesized using a 200×100 cell two-dimensional FD-TD grid having a uniform cell size of 0.5 mm. The broad-band excitation is again a one-half cycle, 3-GHz sinusoidal pulse, TM polarized, and having an incident wavevector oriented at 0° with respect to the $+x$-axis. Time waveforms of the scattered electric near field are observed at the eight points denoted by "+" signs in Fig. 6. Similar to the infinite wedge case, these observation points are causally isolated from diffraction effects at the rear of the strip by proper selection of the size of the FD-TD grid and strip, as well as the number of time steps. This permits the observed fields to decay as they would for an infinitely long strip. Again, the error signal input to the optimizer consists of the square of the sum of the absolute values of the FD-TD computed time samples at the observation points, accumulated until the decay of the computed fields at these points.

To begin the synthesis process for the isotropic coating layers of Case 1, the point ($a_0 = 1, a_1 = -0.4, a_2 = 0, b_0 = 1, b_1 = 1, b_2 = 0$) in the coating six-space is selected arbitrarily as the initial guess. It is found that seven passes through the FD-TD/feedback system are needed for convergence, with each pass requiring 22 FD-TD runs (each 350 time steps). At the conclusion of this process, which involves a total CPU time of 1.2 minutes on a single processor of the Cray X-MP, the operating point in the coating 6-space has shifted to (0.95522, 1.6156, −1.1627, 0.7785, −0.8257, 1.9198), and the error signal has been reduced by a factor of 22:1 from that of the initial guess for the coating.

Fig. 7(a) shows the final coating state for Case 1 after convergence of the synthesis algorithm by plotting the isotropic electric and magnetic conductivity profiles versus layer "j" index. Fig. 7(b) shows the corresponding mitigation of the broad-band scattered pulse in the far field over the bistatic angular range 90°–270°. From Fig. 7(b), we see a moderate level of mitigation, about −20 dB, that is only a weak function of bistatic angle. We also note that the mitigation does not deteriorate appreciably when the incident pulse is rotated by 10° in azimuth.

To begin the synthesis procedure for the anisotropic coating layers of case 2, the point ($c_0 = 1, c_1 = 0, c_2 = 0, d_0 = 1, d_1 = 0, d_2 = 0$) in the coating six-space is selected arbitrarily as the initial guess. It is found that six passes through the FD-TD/feedback system are needed for convergence, with each pass requiring 22 FD-TD runs (each 350 time steps). At the conclusion of this process, which involves a total CPU time of 1.0 min on a single processor of the Cray X-MP, the operating point in the coating six-space has shifted to (1.0299, 0.1299, −0.3277, 4.6508, 4.3234, 6.1330), and the error signal has been reduced by a factor of 240 : 1 from that of the initial guess for the coating.

Fig. 8(a) shows the final coating state for Case 2 after convergence of the synthesis algorithm by plotting the anisotropic electric and magnetic conductivity profiles versus layer "j" index. Fig. 8(b) shows the corresponding mitigation of the broad-band scattered pulse in the far field over the bistatic angular range 90°–270°. From Fig. 8(b), we see that the use of coating anisotropy substantially increases the level of mitigation to the range −35 dB to −38 dB, with the mitigation remaining only a weak function of the bistatic angle. However, similar to the wedge coated with the low-dimensional anisotropic absorber, the sensitivity of the bistatic mitigation to a 10° rotation of the illumination angle (with coating properties fixed at the original synthesized state) is increased relative to the isotropic absorber case. We note, however, that mitigation of the new broad-band monostatic return at 190° improves slightly to −42 dB.

VI. Conclusion

This paper introduced a new time-domain synthesis approach for broad-band absorptive coatings suitable for RCS

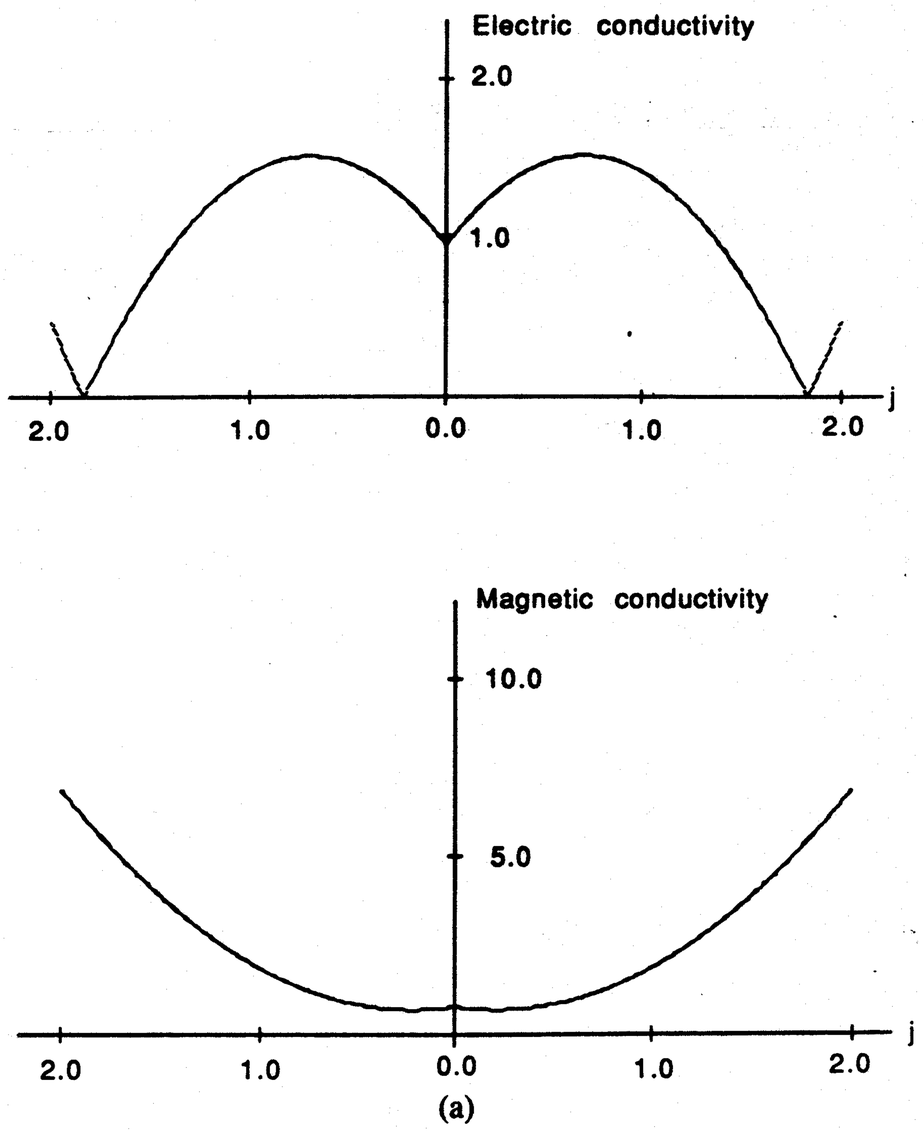

Fig. 7. Synthesis results for the rounded conducting strip, isotropic coating case. (a) Final coating state after convergence of the synthesis algorithm. (b) Mitigation of the broad-band scattered pulse in the far field versus bistatic angle.

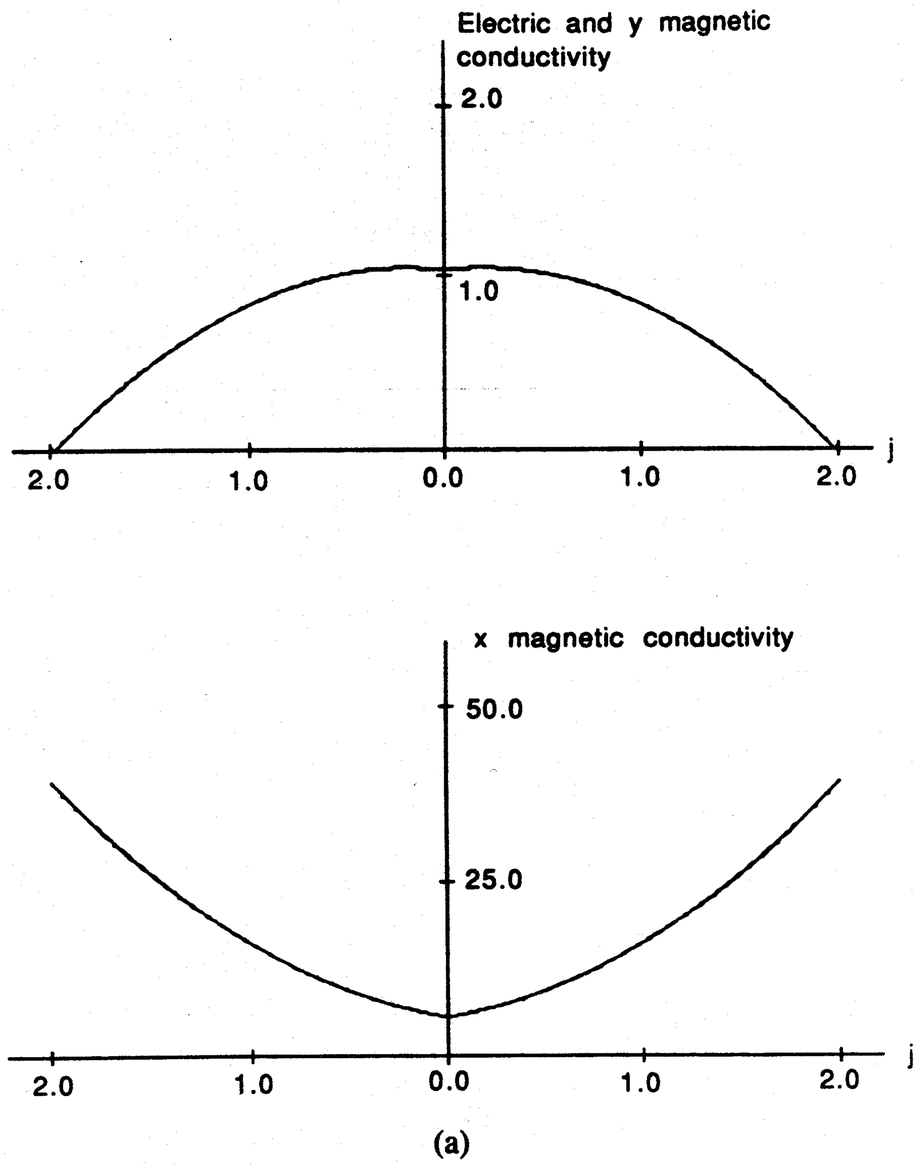

Fig. 8. Synthesis results for the rounded conducting strip, anisotropic coating case. (a) Final coating state after convergence of the synthesis algorithm. (b) Mitigation of the broad-band scattered pulse in the far field versus bistatic angle.

management. The new FD-TD/L-M synthesis algorithm has a number of attractive features. First, the synthesis achieved is just as accurate, flexible, and computationally efficient as the forward-scattering FD-TD element used in the algorithm. Second, the synthesis is broad-band, depending upon the pulsed illumination used, due to the time-domain nature of FD-TD. Third, the synthesis is automated, capable of finding at least locally-optimum coatings in situations where the designer might be faced with many degrees of freedom. Evolution of large-scale concurrent processing, for example using the Connection Machine, to implement efficiently both the FD-TD and nonlinear optimization elements of the algorithm, may permit efficient searches of high-dimensional coating spaces that include manufacturing and economic constraints as well as technical.

ACKNOWLEDGMENT

The authors wish to acknowledge the contributions of Prof. Korada R. Umashankar of the University of Illinois at Chicago in related research involving the formulation of FD-TD/feedback methods for inverse scattering.

REFERENCES

[1] A. Taflove, "Review of the formulation and applications of the finite-difference time-domain method for numerical modeling of electromagnetic wave interactions with arbitrary structures," *Wave Motion*, vol. 10, no. 6, pp. 547–582, Dec. 1988.

[2] D. W. Marquardt, "An algorithm for least-squares estimation of non-

linear parameters," *J. Soc. Indust. Appl. Math.*, vol. 11, no. 2, pp. 431–441, June 1963.

[3] A. Taflove and K. R. Umashankar, "Review of FD-TD numerical modeling of electromagnetic wave scattering and radar cross section," *Proc. IEEE*, vol. 77, pp. 682–699, May 1989.

[4] B. Beker, K. R. Umashankar, and A. Taflove, "Numberical analysis and validation of the combined field surface integral equations for electromagnetic scattering by arbitrary shaped two-dimensional anisotropic objects," *IEEE Trans. Antennas Propagat.*, vol. 37, pp. 1573–1581, Dec. 1989.

[5] M. S. Narasimhan and B. Philips, "Synthesis of near-field patterns of a nonuniformly spaced array," *IEEE Trans. Antennas Propagat.*, vol. AP-35, pp. 1189–1198, Nov. 1987.

[6] K. R. Umashankar and A. Taflove, "A novel method to analyze electromagnetic scattering of complex objects," *IEEE Trans. Electromagn. Compat.*, vol. EMC-24, pp. 397–405, Nov. 1982.

[7] T. G. Moore, A. Taflove, K. R. Umashankar, and B. Beker, "Edge-field behavior for the infinite dielectric wedge: Detailed numerical studies," *IEEE Trans. Antennas Propagat.*, to be submitted.

Mark A. Strickel (S'87–M'88) was born in Chicago, IL, on August 13, 1955. He received the B.S. degree in electrical engineering from the Illinois Institute of Technology, Chicago, in 1983, and the M.S. and Ph.D. degrees in electrical engineering from Northwestern University, Evanston, IL, in 1984 and 1989, respectively.

Between August 1988 and March 1990 he was on the staff of the Institutional Financial Futures and Options Division of Drexel Burnham Lambert. In March 1990, he left Drexel to form his own profit center within Geldermann, Inc., Chicago, IL. His research interests are the development of speculative strategies and financial risk-management techniques using futures and options.

Dr. Strickel is a member of Eta Kappa Nu.

Allen Taflove (M'75–SM'84–F'90), for a photograph and biography please see page 1812 of the December 1988 issue of this TRANSACTIONS.